Compressing surface plasmons for nano-scale optical focusing

Hyeunseok Choi[1,†], David F. P. Pile[1,†], Sunghyun Nam[1], Guy Bartal[1] and Xiang Zhang[1,2]*

[1]NSF Nano-scale Science and Engineering Center, University of California, 5130 Etcheverry Hall, Berkeley, CA 94720, USA
[2]Materials Sciences Division, Lawrence Berkeley National Laboratory, 1 Cyclotron Road, Berkeley, CA 94720, USA
[†] These authors contributed equally to this work.
[*]Corresponding author: xiang@berkeley.edu

Abstract: A major challenge in optics is how to deliver and concentrate light from the micron-scale into the nano-scale. Light can not be guided, by conventional mechanisms, with optical beam sizes significantly smaller than its wavelength due to the diffraction limit. On the other hand, focusing of light into very small volumes beyond the diffraction limit can be achieved by exploiting the wavelength scalability of surface plasmon polaritons. By slowing down an optical wave and shrinking its wavelength during its propagation, optical energy can be compressed and concentrated down to nanometer scale, namely, nanofocusing. Here, we experimentally demonstrate and quantitatively measure the nanofocusing of surface plasmon polaritons in tapered metallic V-grooves down to the deep sub-wavelength scale - $\sim\lambda/40$ at wavelength of 1.5 micron - with almost 50% power efficiency.

References and links

1. S. A. Maier, P. G. Kik, H. A. Atwater, S. Meltzer, E. Harel, B. E. Koel, and A. A. G. Requicha, "Local detection of electromagnetic energy transport below the diffraction limit in metal nanoparticle plasmon waveguides," Nat. Mater. **2**, 229-232 (2003).
2. J. Takahara, S. Yamagishi, H. Taki, A. Morimoto, and T. Kobayashi, "Guiding of a one-dimensional optical beam with nanometer diameter," Opt. Lett. **22**, 475-477 (1997).
3. D. K. Gramotnev, "Adiabatic nanofocusing of plasmons by sharp metallic grooves: geometrical optics approach," J. Appl. Phys. **98**, 104302 (2005).
4. D. F. P. Pile and D. K. Gramotnev, "Adiabatic and nonadiabatic nanofocusing of plasmons by tapered gap plasmon waveguides," Appl. Phys. Lett. **89**, 041111 (2006).
5. D. K. Gramotnev, D. F. P. Pile, M. W. Vogel, and X. Zhang, "Local electric field enhancement during nano-focusing of plasmon by a tapered gap," Phys. Rev. B **75**, 035431 (2007).
6. J. Takahara and F. Kusunoki, "Guiding and nanofocusing of two-dimensional optical beam for nanooptical integrated circuits," IEICE Trans. Electron. **E90–C**, 87-94 (2007).
7. P. Ginzburg, D. Arbel, and M. Orenstein, "Gap plasmon polariton structure for very efficient microscale-to-nanoscale interfacing," Opt. Lett. **31**, 3288-3290 (2006).
8. K. Kurihara, K. Yamamoto, J. Takahara, and A. Otomo, "Superfocusing modes of surface plasmon polaritons in a wedge-shaped geometry obtained by qausi-separation of variables" J. Physics. A: Math. Theor. **41** 195401 (2008).
9. K. V. Nerkararyan, "Superfocusing on a surface polariton in a wedge-like structure," Phys. Lett. A **237**, 103-105 (1997).
10. E. Moreno, S. G. Rodrigo, S. I. Bozhevolnyi, L. Martın-Moreno, and F. J. Garcıa-Vidal, "Guiding and focusing of electromagnetic fields with wedge plasmon polaritons," Phys. Rev. Lett. **100**, 023901 (2008).
11. K. C. Vernon, D. K. Gramotnev, and D. F. P. Pile, "Adiabatic nanofocusing of plasmons by a sharp metal wedge on a dielectric substrate," J. Appl. Phys. **101**, 104312 (2007).
12. A. J. Babadjanyan, N. L. Margaryan, and K. V. Nerkararyan, "Superfocusing of surface polaritons in the conical structure," J. Appl. Phys. **87**, 3785-3788 (2000).
13. M. I. Stockman, "Nanofocusing of optical energy in tapered plasmonic waveguides," Phys. Rev. Lett. **93**, 137404 (2004).

14. N. A. Issa, and R. Guckenberger, "Optical nanofocusing on tapered metallic waveguides," Plasmonics **2**, 31–37 (2007).
15. N. A. Janunts, K. S. Baghdasaryan, K. V. Nerkararyan, and B. Hecht, "Excitation and superfocusing of surface plasmon polaritons on a silver-coated optical fiber tip," Opt. Comm. **253**, 118-124 (2005).
16. W. Ding, S. R. Andrews, and S. A. Maier, "Internal excitation and superfocusing of surface plasmon polaritons on a silver-coated optical fiber tip," Phys. Rev. A **75**, 063822 (2007).
17. E. Verhagen, A. Polman, and L. Kuipers, "Nanofocusing in laterally taperd plasmonic waveguides," Opt. Express **16**, 45-57 (2008).
18. V. S. Volkov, S. I. Bozhevolnyi, S. G. Rodrigo, L. Martin-Moreno, F. J. Garcia-Vidal, E. Devaux, T. W. Ebbesen, "Nanofocusing with channel plasmon polaritons", Nano Lett. **9**, 1278-1282 (2009).
19. T. Yatsui, W. Nomura, and M. Ohtsu, "Metallized slit-shaped pyramidal Si probe with extremely high resolution for 1.5-Tbit/in^2 density near-field optical storage", J. Nanophoton. **1**, 011550 (2007).
20. Z. Liu, J. M. Steele, W. Srituravanich, Y. Pikus, C. Sun, and X. Zhang, "Focusing surface plasmons with a plasmonic lens," Nano Lett. **5**, 726-1729 (2005).
21. Z. Liu, J. M. Steele, H. Lee, and X. Zhang, "Tuning the focus of a plasmonic lens by the incident angle," Appl. Phys. Lett. **88**, 171108 (2006).
22. J. M. Steele, Z. Liu, Y. Wang, and X. Zhang, "Resonant and non-resonant generation and focusing of surface plasmons with circular gratings," Opt. Express **14**, 5664-5670 (2006).
23. W. Srituravanich, L. Pan, Y. Wang, C. Sun, D. B. Bogy, and X. Zhang, "Flying plasmonic lens in the near field for high-speed nanolithography," Nat. Nanotechnol. **3**, 733-737 (2008).
24. Z. Liu, S. Durant, H. Lee, Y. Pikus, N. Fang, Y. Xiong, C. Sun, and X. Zhang, "Far-field optical superlens," Nano Lett. **7**, 403-408 (2007).
25. Y. Xiong, Z. Liu, C. Sun, and X. Zhang, "Two-dimensional imaging by far-field superlens at visible wavelengths," Nano Lett. **7**, 3360-3365 (2007).
26. K. H. Su, Q. H. Wei, and X. Zhang, "Tunable and augmented plasmon resonances of Au/SiO2/Au nanodisks," Appl. Phys. Lett. **88**, 063118 (2006).
27. Y. Liu, G. Bartal, D. A. Genov, and X. Zhang, "Subwavelength discrete solitons in nonlinear metamaterials," Phys. Rev. Lett. **99**, 153901 (2007).
28. R. Oulton, V. Sorger, D. A. Genov, D. F. P. Pile, and X. Zhang, "A hybrid plasmonic waveguide for subwavelength confinement and long range propagation," Nat. Photonics **2**, 496-500 (2008).
29. S. Han, Y. Xiong, D. Genov, Z. Liu, G. Bartal, and X. Zhang, "Ray optics at a deep-subwavelength scale: a transformation optics approach," Nano Lett. **8**, 4243-4247 (2008).

1. Introduction

Nanofocusing is characterized by nano-scale confinement, below the diffraction limit of light, accompanied by enhancement of the intensity or electric field strength. [1,2] Confinement below diffraction limit can be obtained by coupling light to plasma oscillations at a metallic-dielectric surface forming *surface plasmon polaritons* (SPP). [3-29] In particular, a plasmonic waveguide formed by a dielectric gap between two metal half spaces gives rise to a guided mode which does not experience mode cut-off at the nano-scale. [3,4] Consequently, light can be concentrated into the nano-scale, by gradually decreasing the optical waveguide width, which is unattainable in conventional dielectric waveguides. [1,2] This confinement is accompanied by a gradual reduction of the surface-plasmon wavelength due to the unusual dispersion dependence on the thickness of the dielectric gap. Although the optical confinement always comes at the cost of energy dissipation, proper design of plasmonic waveguides enables substantial enhancement of light intensity so that the intensity enhancement overpowers the total power dissipation (Fig. 1a). [5]

Nanofocusing of plasmons was pioneered by Nerkararyan and Stockman on a metallic wedge[9] and metallic cone. [9,13] The growing interest in nano-optics and the advances in nano-fabrication, have led to further theoretical investigations of nanofocusing on the wedge [10,11] and cone [12] as well as in several different plasmonic systems including V-grooves, [3-8] dielectric cones covered in metal film [15,16] and tapered rectangular metal strips. [17] A recent experimental study of plasmons on a rectangular strip of tapered width showed increased photoluminescence in some regions [17] and enhanced fields near tips of tapered channel plasmon waveguides were probed by near-field microscopy. [18] Nanofocusing can also be achieved by plasmonic lens, [20-23] far-field superlens, [24, 25] and other plasmonic systems. [26-29] However, nano-fabrication, detection and excitation difficulties have hindered the experimental verification of the nanofocusing process and its associated properties such as progressive field enhancement and sub-wavelength confinement. While specific applications favor particular nanofocusing structures, V-grooves were theoretically

shown to be promising candidates for achieving maximal field enhancement. [5] Here, we present an experimental evidence for nanofocusing of SPPs in a laterally tapered gap plasmon waveguide, i.e. V-groove. We measure the relative power emerging from V-grooves with different output widths, w, and find the output intensity is increased with decreased output width.
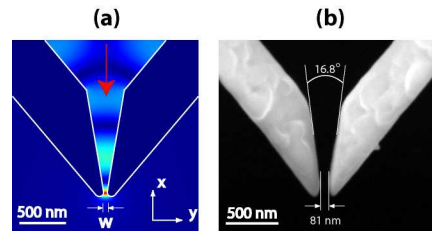
2. Nano-scale V-groove fabrication process

Fig. 1. Illustration of nanofocusing of light. (a) An example of electric field intensity, $|E|^2$, enhancement during nanofocusing in a tapered gap plasmon waveguide illustrates this effect. The electric field is determined by numerical solution of the Maxwell equations for the V-groove output width = 50nm (all other parameters are same as detailed below). (b) Scanning electron microscope image of a typical V-groove's cross-section showing wide upper region for access of the incoming beam and narrow lower region where nanofocusing takes place.

The V-groove fabrication is conducted in metal coated silicon wafers by silicon wet etching and focused ion beam milling. To fabricate deep V-grooves with output gap widths of tens of nanometers, the following process was used (Fig. 2a). We used double side polished silicon wafers (100) of ~350 μm thickness coated with a SiO_2 layer. The SiO_2 layer was patterned by using photolithography and dry etching. We made V-grooves by anisotropic wet etching with KOH solution and the SiO_2 layer, which served as a etch mask, was removed. The depth of the etched silicon V-grooves is deliberately a few microns shorter than the total thickness of the silicon wafer. We then deposited a gold layer of ~ 500 nm thickness on the front side by electron-beam evaporation. Subsequently, a few microns of silicon are etched with XeF_2 dry etching from the backside to expose the metal edge that formed in the removed tip of the silicon V-groove. Then, a smaller V-groove of breadth, *b*, and output width, *w*, is formed by focused ion beam (FIB) milling (Fig. 2). The various output gap widths were obtained by controlling the FIB milling area size, beam current and etching time.

The V-groove structure supported by the silicon wafer provides several advantages over flat free-standing structures in terms of not requiring deposition ultra-thick films for deep V-grooves, deformation- and stress-free films, mechanical strength, etc. The overall structure is a series of aligned V-grooves with varying output widths and fixed breadth of 2 μm. Each V-groove consists of two distinct regions in its cross section; a long and wide upper region of depth 330 μm with grove angle ≈ 70.6°, and a narrow lower region of depth ≈ 950 nm with groove angle ≈ 17° (Fig. 1). We measured several samples with different final gap size and the variation of taper angle is about +/- 1~2 degrees which does not affect our results significantly (according to simulations not shown).

We note that while the metal surface at the upper region can be relatively rough due to the wet etching process, the lower region (which plays the critical role in nanofocusing) is much smoother due to FIB milling, minimizing the scattering losses during the nanofocusing process. A 2 μm breadth, *b* (Fig. 2b), was chosen for all V-grooves, which is (a) sufficiently large compared to the gap plasmon wavelength not to modify the effect of nanofocusing of the fundamental gap plasmon mode and (b) sufficiently small to efficiently suppress existence of higher modes with different strengths of nanofocusing and would result in complex interference patterns.
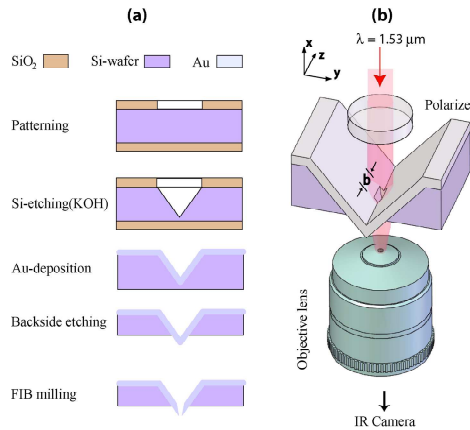
Fig. 2. V-groove fabrication process and optical schematic. (a) Fabrication process for nano scale V-groove. (b) Optical measurement setup for the developed rapid and reliable far-field investigation of nanofocusing.

3. Measurement of nanofocusing effect

To measure the nanofocusing effect, we illuminate simultaneously the wide end of all the V-grooves by a laser beam of vacuum wavelength, λ = 1532 nm, with TM polarization (magnetic field parallel to the z-axis) as shown in Fig. 2b. The incident beam area is sufficiently large to uniformly illuminate all V-grooves of interest. The input width gives rise to propagation of 'photonic modes' (bulk waves in the dielectric) throughout the groove. These modes couple to the gap plasmon mode throughout the propagation (due to the surface roughness), and experience the most efficient coupling at gap width of ~ 770nm where the 'photonic modes' are cut off. The excitation of the gap plasmon mode is confirmed by monitoring strong dependence of the output signal in the input polarization (compare Fig. 3b, TM, and 3c, TE). Since gap plasmons can only be excited for TM polarization[3,4] we should expect plasmon excitation and efficient transmission through the sub-wavelength V-groove output only for TM polarization.
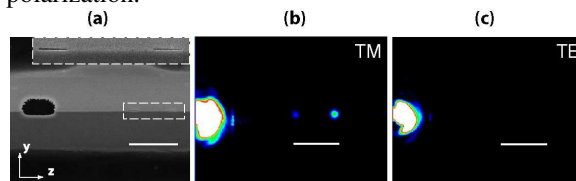

Fig. 3. Illumination by different polarizations of light – plasmon excitation. (a) SEM image of two sub-wavelength width (~100nm) V-groove outputs and a large reference hole as seen from the backside (i.e. looking in the positive *x* direction (Fig. 1a)) together with a magnified view of the V-groove outputs. (b) TM (E-field in the *y*-axis) excitation by the incident laser. (c) Illumination by TE (E-field in the *z*-axis) polarization. Note that the reference hole on the left is sufficiently large to allow both TE and TM wave pass. Scale bars are 10μm.

We measure the output intensity as a function of each groove's minimal width by far-field imaging with a microscope objective lens and an infrared charge-coupled device (CCD) (Fig. 4a, 4c). This measured power at the far-field is then related to the power in the V-groove output, from which the light intensity and the field amplitude in the gaps are deduced. We emphasize that simultaneous uniform illumination and measurement of all the V-grooves with different output widths allows unambiguous verification of the nanofocusing effect through highly reliable comparison among different gap widths.

Figure 4a shows the CCD image of the light radiating from 17 V-groove outputs along with the scanning-electron microscope (SEM) image of the V-groove outputs (Fig. 4b). The encircled four spots in Fig. 4a are in order, from left to right, of descending V-groove output

width. The close-up view of these four spots is given in Fig. 4c. For comparison, we have also numerically calculated the distribution of the square of the electric field amplitude, $|E|^2$, using three-dimensional (3D) finite-difference time-domain (FDTD) solutions. The field distributions calculated in Fig. 4d depict the result of four beams in the four equally illuminated different V-grooves after coupling from the V-groove output and propagating the same distance into free space. We can observe an excellent agreement between the CCD captured images (Fig. 4c) and the calculated distributions (Fig. 4d) at the approximate far-field (red-line in Fig. 4f).

The measured power at the far-field can be related to the light intensity (total power divided by the area) and $|E|^2$ at the V-groove outputs, by calculating the power coupling coefficients from the V-groove output to the far-field. We calculate (not shown here) the coefficients using FDTD, taking the output tip roundness to be r≈50 nm (determined by SEM imaging). The variation of the coupling for different grooves is smaller than 10%, hence, the coupling out does not affect significantly the comparison of intensities measured by the CCD.
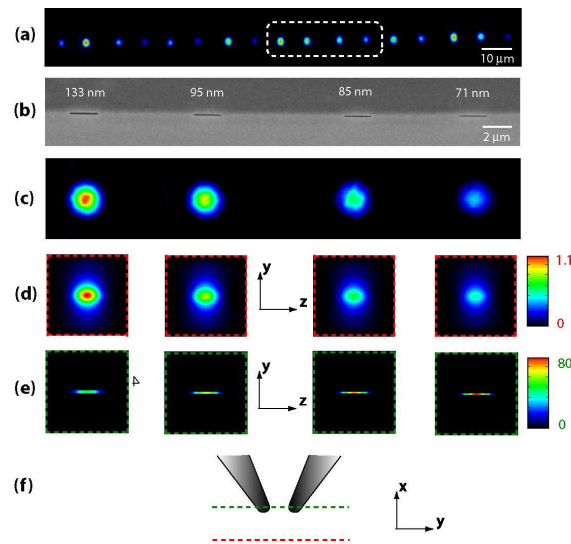

Fig. 4. (a). CCD image of optical output from 17 V-grooves of different output widths. (b) SEM image of the V-groove outputs corresponding to the encircled optical spots in Fig. 4a. (c) Close up view of the CCD image of the four optical spots encircled in Fig. 4a outputted from the structure in Fig. 4b. (d) Calculated square of the electric field amplitude, $|E|^2$ at the approximate far-field (red-line in Fig. 4f). (e) Calculated square of the electric field amplitude, $|E|^2$ at the narrowest part of the V-groove output (green line in Fig. 4f). (f) Schematic for field distributions in Fig. 4d and 4e.

4. Discussion

We quantify the enhancement of the intensity and $|E|^2$ by dividing the measured (relative) values at the grooves outputs by those at a reference plane in which the gap width is 700 nm. The values of the intensity and $|E|^2$ at this plane are readily deduced from the trend of the enhancement with respect to the groove width. The reason for taking 700nm as a (very conservative in terms of predicted enhancement) reference width is two fold: a) this point is close to the free-space diffraction limit of the incident beam. For a fixed optical power, field or intensity enhancement by reducing beam spot size with conventional optics is somewhat arbitrary due to indefinite initial beam spot size. This justifies the use of the plane at which the V-groove width is approximately equal to the diffraction limit as a reference for enhancement. b) The 'photonic mode' supported by the gap structure is cut-off for widths < 770 nm; hence the field in the groove at 700 nm is due to SPP propagation whose enhancement we are interested in.

Figure 5 depicts enhancement of both intensity (a) and $|E|^2$ (b) for all the 17 V-grooves, clearly demonstrating the increase in the enhancement as the gap width is diminished. The results are compared to FDTD simulations, and shows $|E|^2$ enhancement of ~10 for a gap decreasing from 700 nm to 45 nm. We also consider possible variations in simulation parameters which would result in different enhancement during nanofocusing. The dashed curves in Fig. 5b depict the effect of +/- 10 nm variations in the V-groove output width. The experimental and numerically calculated data shows reasonable agreement.

The higher enhancement of peak $|E|^2$ is mainly due to the increase of the ratio $|E/H|$ during the nanofocusing. [5] As both the metal and dielectric structural constituents have no magnetic response, the electric and magnetic fields display a different behavior when the gap is reduced to the nano-scale. While the transverse electric field is confined to the dielectric gap regardless the gap size, the portion of the magnetic field in the metal remains almost unchanged when the gap is decreased. Consequently, the electric field undergoes a more significant enhancement than the magnetic field. This is also related to the increase in the propagation constant (wave-number), which is proportional to the ratio between the electric and magnetic field.
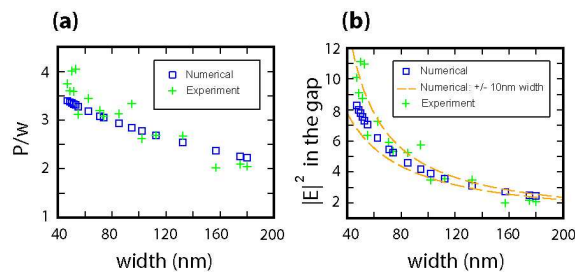

Fig. 5. Intensity and electric field dependence on gap width. (a) In the experiments the guided mode's beam width was scaled down to ~λ/40 (~40nm for λ = 1.53μm). Power (per gap width) dependence on V-groove output width for experiment (crosses) and FDTD simulation (squares). (b) The maximum of $|E|^2$ dependence on V-groove output width from the experimental power (crosses) and FDTD (squares) revealing a measured enhancement of ~10.

5. Conclusions

We have provided experimental verification of the nanofocusing process. The guided mode's beam width was scaled down to ~45 nm which corresponds to ~λ/40 for the wavelength used (λ = 1.53 μm) with a power efficiency of almost 50% (compared to the 700nm reference plane). We measured enhancement of ~10 for the square of the electric field amplitude, $|E|^2$, comparing to the diffraction limit (700 nm beam width), in agreement with theoretical predictions. The peak $|E|^2$ is an important figure of merit for nonlinear optical processes and applications that are electric field dependent, such as Raman spectroscopy and optical lithography. Further localization and enhancement can be achieved by fabrication of smaller V-groove output widths (down to ~1 nm, below which continuous electrodynamics fails). For example, a 2 nm output width can result in enhancement of 421 (comparing very conservatively to a 700nm wide V-groove, and calculated using the same structural parameters and numerical methods used to calculate Figs. 4 and 5). Such enhancements, localization and efficiency render nanofocusing an advantageous tool for a spectrum of nano-optical exploits, such as addressing nano-photonic circuits (or single-molecules and quantum dots), optical nanolithography, non-linear optical sensors, and more.

Acknowledgment